RSC Advances

PAPER

View Article Online
View Journal | View Issue

Open Access Article. Published on 15 June 2022. Downloaded on 10/24/2025 2:38:18 AM.
This article is licensed under a Creative Commons Attribution-NonCommercial 3.0 Unported Licence.

Check for updates

Cite this: *RSC Adv.*, 2022, **12**, 17747

Molecular imprinting as a tool for determining molecular markers: a lung cancer case

Elena Piletska,[a] Kirabo Magumba,[a] Lesslly Joseph,[a] Alvaro Garcia Cruz,[a] Rachel Norman,[b] Rajinder Singh,[b] Antonella F. S. Tabasso,[bc] Donald J. L. Jones,[bde] Salvador Macip[cf] and Sergey Piletsky*[a]

Received 21st March 2022
Accepted 23rd May 2022

DOI: 10.1039/d2ra01830f

rsc.li/rsc-advances

Determining which cancer patients will be sensitive to a given therapy is essential for personalised medicine. Thus, it is important to develop new tools that will allow us to stratify patients according to their predicted response to treatment. The aim of work presented here was to use molecular imprinting for determining the sensitivity of lung cancer cell lines to ionising radiation based on cell surface proteomic differences. Molecularly imprinted polymer nanoparticles (nanoMIPs) were formed in the presence of whole cells. Following trypsinolysis, protein epitopes protected by complexing with MIPs were eluted from the nanoparticles and analysed by LC-MS/MS. The analysis identified two membrane proteins, neutral amino acid transporter B (0) and 4F2 cell-surface antigen heavy chain, the abundance of which in the lung cancer cells could indicate resistance of these cells to radiotherapy. This proof-of-principle experiments shows that this technology can be used in the discovery of new biomarkers and in development of novel diagnostic and therapeutic tools for a personalised medicine approach to treating cancer.

Introduction

Adenocarcinoma is the most common type of non-small lung carcinoma (NSCLC), formed in the mucus making gland cells in the airway's lining.[1–3] It can be treated with surgery, chemotherapy and radiation therapy.[3] Radical radiotherapy is an intensive course that is applied if surgery is not possible.[4] Despite radiotherapy being a useful therapeutic tool, a large proportion of patients experience the recurrence of cancer due to the intrinsic or acquired ability of some cancer cells to resist radiation damage. Lung cancer resistance to radiation contributes largely to disease progression, recurrence and increased cancer mortality.[5]

There are many biological factors implicated in the resistance to ionising radiation (IR), which include redistribution of the cell cycle, repair of DNA damage and apoptosis.[5] The generation of reactive oxygen species (ROS) upon radiation treatment and consequent DNA double-strand breaks contribute to the cytotoxicity of ionisation radiation. Mitochondrial metabolism sustains the redox environment by balancing the production of ROS and their removal by anti-oxidant enzymes. Alterations to protein import and mitochondrial signalling contribute to survival strategies of the tumour cell, giving rise to radioresistance.[6] DNA-dependent protein kinases play a vital role in the non-homologous end-joining repair process and its overexpression has been linked to radiation resistance in glioblastoma cells.[6] Phosphatidylinositol 3-kinase (PI3K/Akt) activation improves cell post-radiation survival by enhancing the repair of DNA double-strand breaks. The overexpression of DNA repair protein RAD51 increases genomic stability, thus influencing radioresistance.[7] Transcription factors including the dynamic NF-κB family proteins and STAT3 contribute to intrinsic radioresistance by producing a variety of proteins including cyclin D1, VEGF and pro-inflammatory cytokines.[7] Prostaglandins derived from Cox-2 protects the cell from damage by ionisation radiation and contribute to the growth and radiation resistance of tumours. Cyclins and cyclin-dependent kinases that control the cell cycle have also been shown to play important roles in the acquisition of radiation resistance.[8]

In the development of radioresistance, the adhesion of a cancer cell to the extracellular matrix (ECM) and communication with surrounding cells plays a significant role, as it influences cell survival in multiple ways. The adhesion of cancerous cells to fibronectin modulates the G2/M arrest, increasing its resistance to the IR. The Notch signalling pathway plays a vital role in cell–cell communication, cell proliferation, stem cell maintenance, cell fate decisions, differentiation and angiogenesis and it positively correlates with poor prognosis

[a]School of Chemistry, College of Science and Engineering, University of Leicester, Leicester, UK. E-mail: sp523@le.ac.uk; Tel: +44-(0)116-0294-4666
[b]Leicester Cancer Research Centre, University of Leicester, Leicester Royal Infirmary, Leicester, UK
[c]Mechanisms of Cancer and Ageing Laboratory, Department of Molecular and Cell Biology, University of Leicester, Leicester, UK
[d]Department of Cardiovascular Sciences, University of Leicester, Leicester, UK
[e]National Institute for Health Research, Leicester Biomedical Research Centre, Glenfield Hospital, Leicester, UK
[f]FoodLab, Faculty of Health Sciences, Universitat Oberta de Catalunya, Barcelona, Spain

© 2022 The Author(s). Published by the Royal Society of Chemistry

Open Access Article. Published on 15 June 2022. Downloaded on 10/24/2025 2:38:18 AM.
This article is licensed under a Creative Commons Attribution-NonCommercial 3.0 Unported Licence.

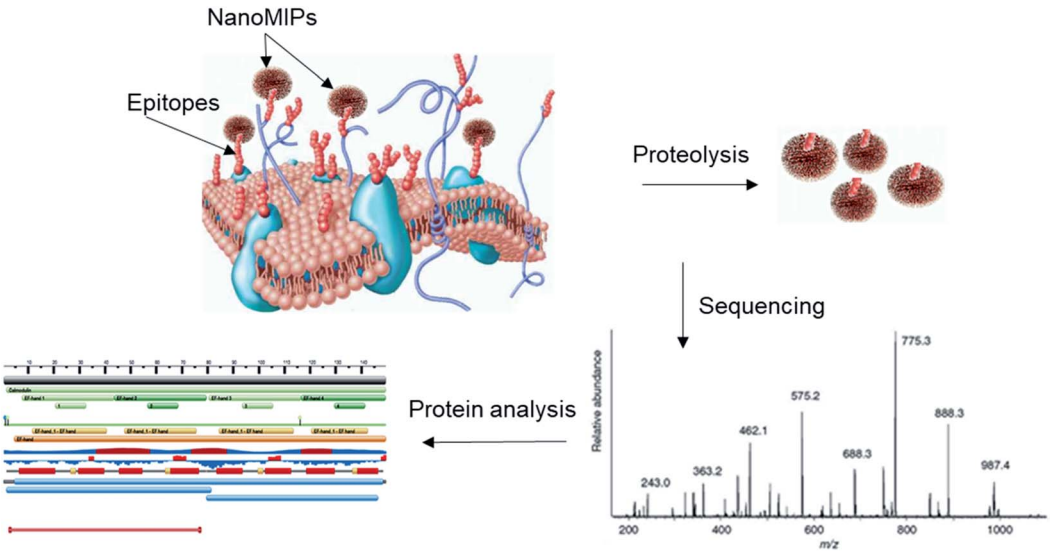

Fig. 1 Steps involved in the use of nanoMIPs for detecting proteins of the surfaceome.

and radioresistance in NSCLC patients.[8] Cell surface receptors, such as integrins mediate the cellular response to the IR and reduce the rate of cell death. Focal adhesion kinase is involved in cellular invasion, motility, proliferation and apoptosis and it contributes to a radioresistant response by activating PI3K-Akt pathway and the induction of many inhibitor of apoptosis proteins.[7–9] The interactions of β1 integrin with paxillin and other proteins is also responsible for the improved survival of radiated cancer cells.[9]

The specific profile of cell surface proteins, known as the surfaceome, is essential to the survival of malignant cells through their involvement in transporting nutrients or ions, cell signalling and adhesion to and/or invasion of tissues or organ surfaces.[10,11] Analysis of their types and abundance can potentially complement tests and scans carried out using computerised tomography, positron emission tomography-computerised tomography, bronchoscopy and biopsy, thus allowing to predict whether Stage 1 and Stage 2 cancers are susceptible to radiation treatment. Plasma membrane cell surface proteins and their epitopes, however, are often difficult to identify because of their low abundance.[11]

Cell surface mapping is a useful research technique in drug development and diagnostics.[12] Typically it consists of "shaving" a significant segment of a cell surface protein by digesting live, intact cells, so the generated peptides can be analysed using LC-MS/MS. The main concern about this approach is identifying surface proteins without the interference of the more abundant cytoplasmic proteins, because when the cell is being digested by trypsin, the cytoplasmic proteins are exposed and are analysed alongside the plasma membrane surface proteins.[12] Since it is difficult to achieve a precise control of experimental conditions in these assays and, for that reason, surfaceome analysis is rarely used in clinical practice.

To address this, for a first time a surfaceome analysis of four lung cancer cells was done using a novel technique of "snapshot imprinting".[13] This technique is based on a phenomenon of molecular imprinting[14,15] that has already earned its place in the biomedical research as an effective tool for diagnostics and imaging.[16–18]

The method involves a formation of nano-molecularly imprinted polymers (nanoMIPs) on the surface of cells by self-assembly of monomers possessing complementary functional groups around the side chains of exposed peptides or "epitopes" followed by polymerisation. The surface peptides capable forming the complexes with nanoparticles are protected against digestion therefore can be eluted from the nanoparticles and then sequenced using standard LC-MS/MS protocols (Fig. 1). Among the benefits of the proposed method are opportunity to compare the surface proteomics of cancer and normal cells, and identify the molecular markers specific for the particular tumours.

Materials and methods

Cell culture

Four non-small cell lung cancer (NSCLC) cell lines were used in this study; A549, H460, H23 and H522. One normal lung fibroblast cell line MRC-5 was also used. Cells were cultured in T75 culture flasks (ThermoFisher, UK) using Roswell Park Memorial Institute 1640 Medium (RPMI) (ThermoFisher, UK) for H460, H23 and H522 cells and Dulbecco's Modified Eagle Medium (DMEM) (ThermoFisher) for A549 cells. All culture medium was supplemented with 10% Fetal Bovine Serum (FBS) (Sigma-Aldrich, UK), unless otherwise stated, and with 1% Penicillin Streptomycin (P/S) (Sigma-Aldrich, UK). Cells were incubated at 37 °C and under 5% CO_2 using a Thermo HeraCell 240 incubator. Cells were routinely checked for mycoplasma contamination. Cells were digested using 0.25% Trypsin–EDTA (Gibco, ThermoFisher, UK) and counted in a haemocytometer before plating for the experiments. All cells were obtained from ATCC.

 © 2022 The Author(s). Published by the Royal Society of Chemistry

Open Access Article. Published on 15 June 2022. Downloaded on 10/24/2025 2:38:18 AM.
This article is licensed under a Creative Commons Attribution-NonCommercial 3.0 Unported Licence.

Colony formation assay

For the colony formation assay or clonogenic assay, cells were seeded at 10^6 in two 6 cm dishes per cell line per dose (0, 2, 4, 6, 8, 10 Gy). The following day, the plates were irradiated at the appropriate doses. The cells were collected and resuspended in media and then counted to be seeded into 6 cm dishes for each dose and cell line to achieve approximately 50 visible colonies at the end of the experiment. The cells were then incubated for 2 weeks. Then, cells were washed with Phosphate Buffered Saline (PBS, Sigma-Aldrich, UK) and fixed using 2 mL of 10% neutral buffered formalin (Fisher, UK). The plates were then washed in PBS and allowed to air dry before the Giemsa staining solution was added and incubated for 5 hours at room temperature. Before imaging the plates were washed with water and counting of colonies was carried out. The Giemsa staining solution was made by mixing 6.4 mL of 67 mM sodium phosphate buffer, pH 7.0, 5 mL of Giemsa stain (Abcam, UK) and water. The phosphate buffer, pH 7.0 was made using 1 : 2 ratio of 1 M monobasic sodium phosphate solution and 1 M dibasic sodium phosphate solution.

Surface mapping

The NCI-H23, NCI-H460, NCI-H522 and A549 cell lines were analysed individually as described earlier.[19] A monomeric mixture was prepared by dissolving 19.5 mg *N*-isopropylacrylamide (NIPAm), 3 mg *N*,*N*′-methylene-bis-acrylamide (MBAA), 15 mg *N-tert*-butylacrylamide (TBAm), and 3 mg 3-aminopropylmethacrylate in 50 mL of PBS and purged with nitrogen for 20 min. The growth media was removed from 250 mL cell culture flasks containing lung cancer cells and cells washed 4 times with 4 × 20 mL of PBS. 30 mL of the monomeric mixture were added to the flasks and polymerisation reaction was initiated by adding 300 μL of freshly prepared solution of 24 mg potassium persulfate and 12 μL of TEMED dissolved in 800 μL of PBS. The polymerisation was carried out for 1 h at room temperature. The mixture was carefully removed from the 250 mL-flasks and cells were washed using 4 × 20 mL of PBS. 3 mg of trypsin (from the bovine pancreas, Sigma T9201), dissolved in 1 mL of PBS, was added to the cell-containing flasks and left for 72 hours at 22 °C. The synthesised nanoMIPs were collected and filtered through a 15 mL Amicon® Ultra centrifugal filter with 100 kDa cut-off (Millipore, UK), at 3500 rpm (2200 g) in order to remove the unreactive functional monomers and cell debris. NanoMIPs were washed on the filter 4 times using 15 mL of PBS, and collected using 1 mL of deionised HPLC water. NanoMIPs were placed in an Eppendorf tube and boiled for 5 min at 98 °C. Sample was filtered through 100 kDa centrifugal filter at 3500 rpm. NanoMIPs were collected again using 1 mL of deionised HPLC water, boiled for 5 minutes at 98 °C and filtered through 100 kDa centrifugal filter at 3500 rpm. This step was repeated three times. The solution of the eluted peptides was collected, lyophilised and sent off for sequencing.

LC-MS/MS analysis

Samples were reconstituted in 20 μL 0.1% formic acid, 3% acetonitrile and 20 μL of 100 fmol alcohol dehydrogenase (ADH) then transferred to HPLC vials. The known amount of ADH protein allowed the peptides to be quantified in the sample by comparing peak areas. Samples were treated using a Waters nanoACQUITY UPLC using Waters 2G-V/M Symmetry C18 trap column (180 μm × 20 mm, 5 μm), to focus the peptides before elution onto the LC column and injected into Waters Acquity HSS T3 analytical UPLC column (75 μm × 250 mm, 1.8 μm). Trapping method: single pump trapping with 99.9% solvent A and 0.1% solvent B at a flow rate of 5 μL min^{-1} for 3 min. Analytical column gradient: 0 min- 3% B, 30 min – 40% B, 32 min - 85% B, 40 min - 85% B and 41 min - 3% B. The flow rate was 0.3 μL min^{-1} and the temperature of the column was 40 °C. (Solvent A = LC-MS grade water with 0.1% formic acid and Solvent B = acetonitrile with 0.1% formic acid). The NanoAcquity UPLC was coupled to a Waters Synapt G2 HDMS mass spectrometer used in positive electrospray ionisation mode. Capillary voltage = 2.4 kV, cone voltage = 30 V. A helium gas flow of 180 mL min^{-1} and ion mobility separator nitrogen gas flow of 90 mL min^{-1} with a pressure of 2.5 mbar were used. The IMS wave velocity was set at 650 m s^{-1} and the IMS wave height at 40 V. [Glu1]-fibrinopeptide (GFP) with *m*/*z* 785.8427 was used as a lockspray to maintain mass accuracy. Argon was used as the collision gas. For low energy acquisition, the collision energy was set at 4 V and for high energy acquisition, a voltage gradient from 20–40 V was used. Data was acquired using the MassLynx 4.1 software. Raw data was analysed using Progenesis QI for proteomics (Non-Linear Dynamics (Waters), UK). This aligns the chromatography for each run to one selected run, performs peak picking and identifies peptides and proteins from the peptide and fragment *m*/*z* values and searching against a human database from UniProt (downloaded in 2017). A between-subject experiment design was used to compare resistant and sensitive cell lines. The method was repeated to compare resistant cell lines against each other and sensitive cell lines against each other.

Dynamic light scattering analysis

The diameter of nanoMIPs was measured in water using Zetasizer, Nano Series (Malvern, UK). 1 mL of the nanoparticles sample was briefly sonicated using ultrasonic bath and measured for six cycles comprising 14 measurements in the disposable cuvettes at 25 °C.

Transmission electron microscopy (TEM) of the nanoMIP samples

Transmission electron microscopy (TEM) images were obtained in a JEOL JEM-1400 TEM with an accelerating voltage of 120 kV, equipped with EMSIS Xarosa digital camera with Radius software. Samples were sonicated for 2 min immediately prior to adsorption to the grid. Then, 10 μL of the sample was applied to a freshly glow discharged carbon film grid (400 mesh, AGS160-Agar Scientific Ltd). Grids were glow discharged in a Quorum GloQube System for 15 s at 20 mA. Then, the sample was left to adsorb and dry for 25 min at a room temperature. The statistical analysis of the images was made using open source software ImageJ.

Open Access Article. Published on 15 June 2022. Downloaded on 10/24/2025 2:38:18 AM.
This article is licensed under a Creative Commons Attribution-NonCommercial 3.0 Unported Licence.

Results and discussion

The analysis of the surface proteome by the "shaving" approach is gaining popularity, and it has been employed in analysis of cells from more than 20 different species, both prokaryotic and eukaryotic.[20] It is particularly valuable for identifying arrays of surface-exposed proteins that can be used in the development of novel vaccines, drugs or in diagnostics. It has, however, two limitations. First, approximately half of the proteins identified by shaving are actually cytoplasmic proteins, which authors refer to as "non-classical secreted proteins". In addition, there is a disconnect between the epitope abundance on cell membrane and the immunodominance hierarchy of identified epitopes.[21] It would be ideal if the protocol applied in surfaceome analysis could provide also an information about the ability of identified epitopes to generate antibodies or synthetic binders.

NanoMIPs represent a new class of compounds that can be deployed to detect extracellular protein targets (as an alternative to biological antibodies), and potentially currently inaccessible intracellular proteins.[22] Studies suggested that cross-linking of the polymer in the presence of cells leads to the organisation of the polymer chains around the phospholipid and protein templates, such that the geometrical and chemical information of the cell surface is captured by the polymer.[23] Extraction of this information is possible by combining molecular imprinting and proteomics. Recently, we have shown that molecular imprinting can be used to obtain accurate information about peptide epitopes expressed on the surface of a single protein.[14] In this work, we expanded this protocol towards identification of proteins (and their epitopes involved in production of nanoMIPs), expressed on the surface of whole cells.

It is possible to visualise cell imprinting as "freezing" exposed fragments of cell proteins in their complex with polymeric networks. This allows performing subsequent cell lysis without worrying whether cells remain intact during trypsinolysis. The removal of peptides belonging to cytoplasmic proteins from synthesised nanoMIPs can be achieved by simple washing. As model systems for this work, we selected four lung cancer cell lines: A549 and NCI-H460, which show some resistance to ionising radiation and NCI-H23 and NCI-H522, which are more sensitive than the other two cell lines (Fig. 2).

There are the steps taken for identification of membrane proteins in surfaceome analysis by using molecular imprinting. Live cells were used as templates in formation of molecularly imprinted polymer nanoparticles (nanoMIPs). The four types of lung cancer cells were imprinted as described in the Experimental section. Comparison of epitope and protein sets identified for four cell lines might identify cross-reactive epitopes, help avoid molecular mimicry, and elucidate novel insights into mechanisms of cell resistivity to ionisation radiation.[18] The polymerisation of nanoparticles was performed in relatively mild conditions that did not cause cell lysis.[19]

In theory, since monomers and initiators cannot penetrate inside cells during the short time of the polymerisation reaction, only epitopes of the proteins exposed on the cell surface contributed to the formation of nanoMIPs. Trypsin was used to digest the proteins, releasing from the cells nanoMIPs with fragments of proteins protected by their interactions with the polymeric nanoparticle. Next, nanoMIPs were washed from the cell debris followed by several cycles of centrifugation using filtration cartridges. Peptide epitopes were then eluted, concentrated and sequenced by LC-MS/MS. The epitopes sequences were analysed providing information about types of the proteins exposed on cell membranes, and which contributed to the formation of nanoMIPs, and their abundance.[19]

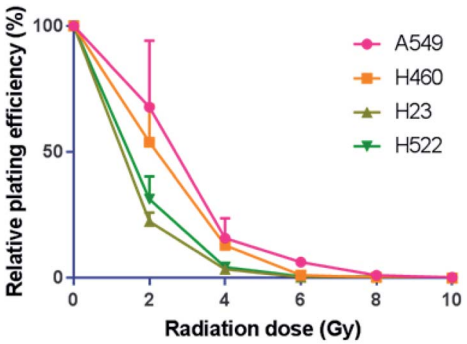

Fig. 2 Different sensitivity of NSCLC cell lines to radiation. Relative plating efficiency (represented as percentage of surviving colonies relative to the control) for colony formation assays of A549, H460, H23 and H522 cells exposed to various amounts of radiation (0, 2, 4, 6, 8 or 10 Gy). Data represents the mean and standard deviation of three independent experiments.

After elution of the peptides nanoMIPs were characterised using DLS. It was found that the diameter of the nanoMIPs in water was on average 98 nm ± 14 nm (polydispersity index – 0.2). This size corresponds to the value reported for nanoMIPs imprinted with proteins.[24] The typical appearance of the nanoMIPs under the TEM is shown on the Fig. 3; the size measured using ImageJ was 54 nm ± 11 nm.

The data produced from regular LC-MS/MS analysis shows presence of both, membrane and non-membrane proteins (Tables 1 and 2).

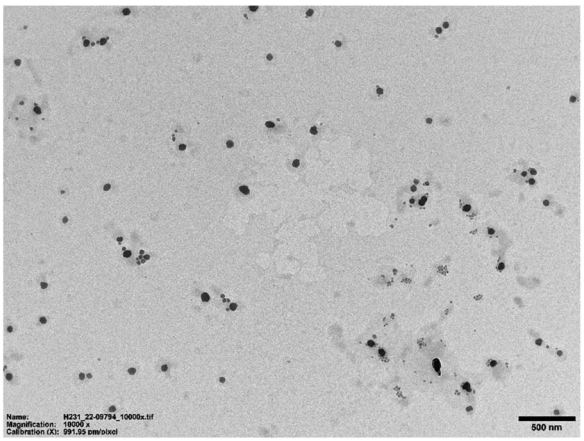

Fig. 3 TEM image of the nanoMIPs obtained after surface mapping of H23 cell line (magnification – 10 000×).

 © 2022 The Author(s). Published by the Royal Society of Chemistry

Open Access Article. Published on 15 June 2022. Downloaded on 10/24/2025 2:38:18 AM.
This article is licensed under a Creative Commons Attribution-NonCommercial 3.0 Unported Licence.

Table 1 Proteins found in the H23 and H460 cell lines. Data show average values for the experiments repeated in triplicate. STD: standard deviation. Location is based on UniProtKB predictions

Description	H23 average amount (fmol)	STD	H460 average amount (fmol)	STD	Location
Translational activator of cytochrome c oxidase 1	34.7	32.3	153.6	9.9	Mitochondrion
ATP synthase subunit O, mitochondrial	23.8	2.4	58.8	12.1	Mitochondrion
Cytochrome c oxidase subunit 5B, mitochondrial	13.8	0.9	30.4	3.2	Mitochondrion
Zinc phosphodiesterase ELAC protein 2	0.7	0.8	19.4	4.2	Mitochondrion
Cytochrome b-c1 complex subunit 2, mitochondrial	6.0	0.3	14.7	0.7	Mitochondrion
Succinate dehydrogenase [ubiquinone] flavoprotein subunit, mitochondrial	1.4	0.7	4.7	0.2	Mitochondrion
Sideroflexin-3	3.7	1.0	1.1	0.4	Mitochondrion
RNA-binding protein 25	2.0	0.3	31.2	4.7	Nucleus
Zinc finger protein 670	61.3	0.8	16.0	2.0	Nucleus
Zinc finger protein 454	2.6	0.3	5.6	2.5	Nucleus
Galectin-12	2.1	1.0	0.7	0.1	Nucleus
DNA-binding protein RFX5	8.5	0.7	0.8	0.5	Nucleus
Galectin-3	22.4	1.4	0.0	0.0	Nucleus
Protein argonaute-1	2.3	0.7	59.7	9.6	Nucleus
Neutral amino acid transporter B (0)	6.7	0.4	20.2	1.2	Plasma membrane
4F2 cell-surface antigen heavy chain	0.2	0.2	3.0	0.8	Plasma membrane
RELT-like protein 1	0.4	0.2	1.1	0.7	Plasma membrane
Ezrin	83.1	3.0	0.0	0.0	Plasma membrane
Protein disulfide-isomerase A6	1.0	0.3	7.9	0.5	Endoplasmic reticulum
Calnexin	35.1	1.1	4.0	0.7	Endoplasmic reticulum
Kinesin light chain 3	13.0	0.9	33.5	3.5	Cytoskeleton
Rootletin	10.9	0.6	0.4	0.3	Cytoskeleton
TNF receptor-associated factor 2	12.4	0.2	5.8	2.0	Cytoplasm
Angiopoietin-2	5.4	0.6	0.8	0.4	Extracellular

It is essential that by the nature of molecular imprinting, every epitope discovered in this study (and used for protein identification) will be able to generate high affinity nanoMIPs. The number of proteins identified post trypsinolysis is slightly smaller than these in the shaving approach (23–35 *versus* 41–51).[11,25] It is possible that the efficiency of the protease treatment is affected by the presence of nanoMIPs on cell surface. This is in agreement with experiments performed using immobilised trypsin, where the number of identified proteins was similar (31 proteins).[25] Approximately 60% of identified proteins are found in all cells tested here, albeit their quantities varied from cell to cell. It is interesting that the fraction of epitopes of cytoplasmic proteins present in the samples is relatively small. The majority of proteins identified in this experiment belong to "bound" proteins located in mitochondrion, nucleus or plasma membranes (Tables 1 and 2).

It has been proposed that in proteolytic "shaving", only approximately half of the identified proteins actually belong to membrane proteins.[26] To explain this phenomenon authors presented the following hypotheses: (i) cytoplasmic proteins come from cell lysis, thus contaminating the "surfaceome" fraction; (ii) cytoplasmic proteins have reached the surface by unspecified exporting/secretory machinery. Whether cytoplasmic proteins without any canonical secretion/exporting or retention signal are really translocated across the membrane is still unresolved, although there are many evidences both in prokaryotes and eukaryotes.[27–29]

The proportion of predicted proteins present in surfaceome analyses vary even among different strains of the same species. Therefore, in the search of potential biomarkers of cell resistance to ionisation radiation, we have looked only at proteins identified by abundance of peptide epitopes in both resistant lines, NCI-H460 and A549, as compared to NCI-H23 and NCI-H522. Predicted cytoplasmic proteins could be considered as remaining contamination from residual cell lysis, and therefore discarded from the following discussion.

The comparison between the surfaceome of resistant and sensitive cell lines allowed us to propose potential biomarkers of radiation resistance based on their relative specific amounts (Table 3). Specifically, neutral amino acid transporter B (0) and 4F2 cell-surface antigen heavy chain are present in larger quantities in radiation resistant cells when compared to cells sensitive to radiation.

Neutral amino acid transporter B (0) is coded by the SLC1A5 gene, also known as ASCT2. ASCT2 is a glutamine transporter belonging to the SLC1 family.[30] Glutamine promotes cancer cell proliferation, and is transported in a Na^+-dependent manner.[31,32] SLC1A5/ASCT2 is highly expressed in various cancer cells, including lung cancer where it is required for cell growth and survival.[32] In NSCLC, ASCT2 is associated with tumour aggressiveness, prognosis and metastasis and its

Open Access Article. Published on 15 June 2022. Downloaded on 10/24/2025 2:38:18 AM.
This article is licensed under a Creative Commons Attribution-NonCommercial 3.0 Unported Licence.

Table 2 Proteins found in the A549 and H522 cell lines. Data show average values for the experiments repeated in triplicate. STD: standard deviation. Location is based on UniProtKB predictions

Description	A549 average amount (fmol)	STD	H522 average amount (fmol)	STD	Location
Trifunctional enzyme subunit alpha, mitochondrial	1053.1	15.9	244.0	174	Mitochondrion
Translational activator of cytochrome c oxidase 1	322.6	6.6	104.1	61.3	Mitochondrion
28S ribosomal protein S35, mitochondrial	41.9	3.6	10.9	8.0	Mitochondrion
Cytochrome c oxidase subunit 5B, mitochondrial	78.6	17.4	3.5	1.6	Mitochondrion
Malate dehydrogenase, mitochondrial	64.1	7.9	2.3	1.3	Mitochondrion
Single-stranded DNA-binding protein, mitochondrial	33.3	1.1	1.9	0.7	Mitochondrion
ADP/ATP translocase 1	32.3	1.5	0.5	0.3	Mitochondrion
ATP synthase subunit O, mitochondrial	64.0	6.7	0.4	0.4	Mitochondrion
Cytochrome c oxidase subunit 6C	27.0	1.7	0.3	0.2	Mitochondrion
NADH dehydrogenase [ubiquinone] 1 beta subcomplex subunit 4	24.1	4.4	0.2	0.1	Mitochondrion
ATP synthase F(0) complex subunit B1, mitochondrial	17.4	2.8	0.0	0.0	Mitochondrion
Sideroflexin-3	12.4	2.5	0.0	0.0	Mitochondrion
Succinate dehydrogenase [ubiquinone] flavoprotein subunit, mitochondrial	11.9	1.0	0.0	0.0	Mitochondrion
UDP-glucose 6-dehydrogenase	448.8	6.8	2163.2	1060	Nucleus
2′-5′-Oligoadenylate synthase 1	60.1	3.1	3.3	2.5	Nucleus
SRA stem-loop-interacting RNA-binding protein, mitochondrial	60.3	25.6	3.0	1.1	Nucleus
Pyruvate kinase PKM	78.2	5.0	2.9	1.1	Nucleus
Nucleic acid dioxygenase ALKBH1	32.2	1.2	1.1	0.6	Nucleus
DNA-binding protein RFX5	41.1	3.6	0.2	0.1	Nucleus
EP300-interacting inhibitor of differentiation 1	60.5	12.8	0.0	0.0	Nucleus
Galectin-12	26.7	3.2	0.0	0.0	Nucleus
Heterogeneous nuclear ribonucleoprotein K	10.6	1.9	0.0	0.0	Nucleus
Galectin-3	5.47	0.17	0.0	0.00	Nucleus
Aspartate aminotransferase, mitochondrial	7.1	0.2	20.2	4.5	Plasma membrane
Neutral amino acid transporter B (0)	27.5	5.7	2.3	2.2	Plasma membrane
RELT-like protein 1	60.7	2.8	1.8	1.5	Plasma membrane
4F2 cell-surface antigen heavy chain	9.1	0.2	0.0	0.8	Plasma membrane
Ezrin	55.0	2.7	0.0	0.0	Plasma membrane
Calnexin	106.5	9.2	4.0	0.7	Endoplasmic reticulum
Dolichyl-diphosphooligo-saccharide-protein glycosyltransferase subunit 1	15.8	3.6	0.3	0.2	Endoplasmic reticulum
Epoxide hydrolase 1	31.2	0.9	8.4	4.2	Endoplasmic reticulum
ADP-ribosylation factor GTPase-activating protein 2	266.6	5.2	25.6	5.0	Golgi apparatus
Alcohol dehydrogenase 1	144.5	5.9	416.8	130	Cytoplasm
Profilin-1	21.6	3.4	3.7	2.1	Cytoskeleton
Angiopoietin-2	5.4	0.6	0.8	0.4	Extracellular

Table 3 Presence of potential biomarkers or radiation resistance in the lung cancer cell lines

	Average amount, fmol				
Description	H23	H522	H460	A549	Max fold change
Neutral amino acid transporter B (0)	6.7	2.3	20.2	27.5	>3
4F2 cell-surface antigen heavy chain	0.2	0.04	3.0	9.1	>15

 © 2022 The Author(s). Published by the Royal Society of Chemistry

Open Access Article. Published on 15 June 2022. Downloaded on 10/24/2025 2:38:18 AM. This article is licensed under a Creative Commons Attribution-NonCommercial 3.0 Unported Licence.

expression in a adenocarcinomas is associated with disease stage, cell proliferation and angiogenesis.[31] Because all this, the SLC1A5 gene that codes neutral amino acid transporter B (0) could be used as a potential diagnostic and therapeutic target.[31,32]

4F2 antigen heavy chain, also known as CD98 heavy chain, is encoded by the SLC3A2 gene. CD98 heavy chain mediates cell adhesion, motility, growth, and survival by binding to β-integrin.[33] The overexpression of CD98 has been identified as an oncogenic driver of proliferation and invasion and it has been classed as a negative prognostic factor in NSCLC.[33]

Verification of these proteins as true biomarkers of radiation resistance requires more efforts and should be performed using multiple biopsy samples. This is obviously outside of the scope of present work, which was aimed at developing a fast and reliable way to compare a set of surface proteins by combining molecular imprinting and proteomic analysis. This novel approach cannot possibly substitute other protocols used in the fundamental research of the surfaceome. Instead, it can offer alternative ways for the reduction of the initial set of candidates to be explored in a surfaceome analysis. A strong advantage of the proposed approach lies in the possibility to perform quick and simple analysis of cell lines for the presence of protein markers. This means that, for the first time, surfaceome analysis could be used in clinical practice (following further optimisation and validation work). In addition, this approach allows identification of peptide epitopes that have very high probability to generate high affinity binders, such as MIPs and, possibly, antibodies. By the nature of molecular imprinting, every epitope discovered in this study was able to generate high affinity nanoMIPs. This is in contrast to established protocols where information obtained about peptides/protein structure (*e.g.* in the "shaving" approach) cannot be used for generating antibodies due to lack of correlation between abundance of proteins and their immunogenicity. Thus, nanoMIPs synthesised for identified epitopes can be used for selective targeting cancer cells and other types of cells, and provide novel potential diagnostic and therapeutic tools.[34–37]

Conclusions

The experiments undertaken to analyse lung cancer cell lines by molecular imprinting were successful in identifying differences in their surfaceome. The optimised method generated reproducible results. Some variations in the concentrations of the proteins were different in each repeat due to the differences in the growth stage of the cells. Nevertheless, they were consistent with being overexpressed in one cell line over the others. The presence of cytoplasmic proteins in surfaceome samples is in line with observations made earlier. We propose that the cell surface proteins neutral amino acid transporter B (0) and 4F2 cell-surface antigen heavy chain could be used as biomarkers for NSCLC resistance to ionisation radiation. In conclusion, the experimental method conducted in this project provided several proteins that could be investigated for how lung cancer cells acquire and maintain resistance to radiotherapy. The epitopes and proteins identified in our work can be used for cancer diagnostics and treatments. The proposed novel approach allows to shorten the timetable to discover new candidates, compared to the classical, pre-genomics methods.

Conflicts of interest

There are no conflicts of interest to declare.

Author contributions

Elena Piletska: investigation, Analysis, writing – review & editing. Kirabo Magumba: methodology, investigation, Lesslly Joseph: methodology, investigation. Alvaro Garcial Cruz: TEM analysis. Rachel Norman: investigation. Rajinder Singh: formal analysis. Antonella F. S. Tabasso: investigation. Donald J. L. Jones: methodology. Salvador Macip: methodology, Supervision. Sergey A. Piletsky: conceptualization, formal analysis, writing – original draft.

References

1 H. Lemjabbar-Alaoui, O. U. I. Hassan, Y.-W. Yang and P. Buchanan, *Biochim. Biophys. Acta, Rev. Cancer*, 2015, **1856**, 189–210.
2 S. Moore, *Cancer Nurs. Pract.*, 2010, **9**, 11.
3 G. L. Patrick, *An Introduction to Medicinal Chemistry*, Oxford Univ. Press, 2009.
4 S. Baker, M. Dahele, F. J. Lagerwaard and S. Senan, *Radiat. Oncol.*, 2016, **11**, 115.
5 Y. Liu, X. Chen, Q. Hu, J. Huang and C. Ling, *Int. J. Clin. Exp. Med.*, 2018, **11**, 7628–7676.
6 B. Kim, Y. Hong, S. Lee, P. Liu, J. Lim, Y. Lee, T. Lee, K. Chang and Y. Hong, *Int. J. Mol. Sci.*, 2015, **16**, 26880–26913.
7 A. Laine, P. Iyengar and T. K. Pandita, *Mol. Cancer Res.*, 2013, **11**, 967–972.
8 J. Theys, S. Yahyanejad, R. Habets, P. Span, L. Dubois, K. Paesmans, B. Kattenbeld, J. Cleutjens, A. J. Groot, O. C. J. Schuurbiers, P. Lambin, J. Bussink and M. Vooijs, *Radiother. Oncol.*, 2013, **108**, 440–445.
9 J. Seidler, R. Durzok, C. Brakebusch and N. Cordes, *Radiother. Oncol.*, 2005, **76**, 129–134.
10 R. Hynes, *Biochim. Biophys. Acta, Rev. Cancer*, 1976, **458**, 73–107.
11 A. Olaya-Abril, I. Jiménez-Munguía, L. Gómez-Gascón and M. J. Rodríguez-Ortega, *J. Proteomics*, 2014, **97**, 164–176.
12 R. L. Juliano and V. Ling, *Biochim. Biophys. Acta*, 1976, **455**, 152–162.
13 S. A. Piletsky, E. V. Piletska, F. Canfarotta and D. Jones, *Methods and kits for determining binding sites*, WO2018178629A1, 2018.
14 L. Chen, X. Wang, W. Lu, X. Wu and J. Li, *Chem. Soc. Rev.*, 2016, **45**, 2137–2211.
15 M. Arabi, A. Ostovan, J. Li, X. Wang, Z. Zhang, J. Choo and L. Chen, *Adv. Mater.*, 2021, **33**, e2100543.
16 E. V. Piletska, A. Guerreiro, M. Mersiyanova, T. Cowen, F. Canfarotta, S. Piletsky, K. Karim and S. Piletsky, *Langmuir*, 2020, **36**, 279–283.

Open Access Article. Published on 15 June 2022. Downloaded on 10/24/2025 2:38:18 AM.
This article is licensed under a Creative Commons Attribution-NonCommercial 3.0 Unported Licence.

17 K. G. Shevchenko, I. S. Garkushina, F. Canfarotta, S. A. Piletsky and N. A. Barlev, *RSC Adv.*, 2022, **12**, 3957–3968.
18 M. Jia, Z. Zhang, J. Li, X. Ma, L. Chen and X. Yang, *TrAC Trends Anal. Chem.*, 2018, **106**, 190–201.
19 S. S. Piletsky, E. Piletska, M. Poblocka, S. Macip, D. J. L. Jones, M. Braga, T. H. Cao, R. Singh, A. C. Spivey, E. O. Aboagye and S. A. Piletsky, *Nano Today*, 2021, **41**, 101304.
20 A. Olaya-Abril, I. Jiménez-Munguía, L. Gómez-Gascón and M. J. Rodríguez-Ortega, *J. Proteomics*, 2014, **97**, 164–176.
21 F. Canfarotta, A. Waters, R. Sadler, P. McGill, A. Guerreiro, D. Papkovsky, K. Haupt and S. Piletsky, *Nano Res.*, 2016, **9**, 3463–3477.
22 D. Yongabi, M. Khorshid, P. Losada-Pérez, K. Eersels, O. Deschaume, J. D'Haen, C. Bartic, J. Hooyberghs, R. Thoelen, M. Wübbenhorst and P. Wagner, *Sens. Actuators, B*, 2018, **255**, 907–917.
23 R. Liu, A. M. Enstrom and K. S. Lam, *Exp. Hematol.*, 2003, **31**, 11–30.
24 J. Xu, P. X. Medina-Rangel, K. Haupt and B. Tse Sum Bui, *Methods Enzymol.*, 2017, **590**, 115–141.
25 H. Tjalsma, L. Lambooy, P. W. Hermans and D. W. Swinkels, *Proteomics*, 2008, **8**, 1415–1428.
26 L. Gómez-Gascón, I. Luque, A. Olaya-Abril, I. Jiménez-Munguía, R. A. Orbegozo-Medina, E. Peralbo, C. Tarradas and M. J. Rodríguez-Ortega, *J. Proteomics*, 2012, **75**, 5654–5666.
27 L. Aguilera, E. Ferreira, R. Giménez, F. J. Fernández, M. Taulés, J. Aguilar, M. C. Vega, J. Badia and L. Baldomà, *Int. J. Biochem. Cell Biol.*, 2012, **44**, 955–962.
28 J. D. Bendtsen, L. Kiemer, A. Fausbøll and S. Brunak, *BMC Microbiol.*, 2005, **5**, 58.
29 C. Nombela, C. Gil and W. L. Chaffin, *Trends Microbiol.*, 2006, **14**, 15–21.
30 L. Pochini, M. Scalise, M. Galluccio and C. Indiveri, *Front. Chem.*, 2014, **2**, 61.
31 K. Shimizu, K. Kaira, Y. Tomizawa, N. Sunaga, O. Kawashima, N. Oriuchi, H. Tominaga, S. Nagamori, Y. Kanai, M. Yamada, T. Oyama and I. Takeyoshi, *Br. J. Cancer*, 2014, **110**, 2030–2039.
32 M. Hassanein, M. D. Hoeksema, M. Shiota, J. Qian, B. K. Harris, H. Chen, J. E. Clark, W. E. Alborn, R. Eisenberg and P. P. Massion, *Clin. Cancer Res.*, 2013, **19**, 560–570.
33 C. Ocklind, U. Forsum and B. Obrink, *J. Cell Biol.*, 1983, **96**, 1168–1171.
34 A. Cecchini, V. Raffa, F. Canfarotta, G. Signore, S. Piletsky, M. P. MacDonald and A. Cuschieri, *Nano Lett.*, 2017, **17**, 2307–2312.
35 F. Canfarotta, L. Lezina, A. Guerreiro, J. Czulak, A. Petukhov, A. Daks, K. Smolinska-Kempisty, A. Poma, S. Piletsky and N. A. Barlev, *Nano Lett.*, 2018, **18**, 4641–4646.
36 P. Shende, S. Augustine, B. Prabhakar and R. S. Gaud, *Expert Rev. Mol. Diagn.*, 2019, **19**, 409–417.
37 A. E. Ekpenyong-Akiba, F. Canfarotta, B. Abd H, M. Poblocka, M. Casulleras, L. Castilla-Vallmanya, G. Kocsis-Fodor, M. E. Kelly, J. Janus, M. Althubiti, E. Piletska, S. Piletsky and S. Macip, *Nanoscale Horiz.*, 2019, **4**, 757–768.

 © 2022 The Author(s). Published by the Royal Society of Chemistry